Possibility for a full optical determination of photodynamic therapy outcome

J. D. Vollet-Filho,[1] P. F. C. Menezes,[1] L. T. Moriyama,[1] C. Grecco,[1] C. Sibata,[2] R. R. Allison,[2] O. Castro e Silva, Jr.,[1] and V. S. Bagnato[1,a)]
[1]*Instituto de Física de Sao Carlos, University of Sao Paulo (IFSC/USP), Av. Trabalhador Saocarlense, 400 Cx. Postal 369, CEP 13560-970, Sao Carlos, SP, Brazil*
[2]*Department of Radiation Oncology, Leo Jenkins Cancer Center, Brody School of Medicine, East Carolina University, East Fifth Street, Greenville, North Carolina 27858-4353, USA*

(Received 16 April 2008; accepted 16 November 2008; published online 19 May 2009)

The efficacy of photodynamic therapy (PDT) depends on a variety of parameters: concentration of the photosensitizer at the time of treatment, light wavelength, fluence, fluence rate, availability of oxygen within the illuminated volume, and light distribution in the tissue. Dosimetry in PDT requires the congregation of adequate amounts of light, drug, and tissue oxygen. The adequate dosimetry should be able to predict the extension of the tissue damage. Photosensitizer photobleaching rate depends on the availability of molecular oxygen in the tissue. Based on photosensitizers photobleaching models, high photobleaching has to be associated with high production of singlet oxygen and therefore with higher photodynamic action, resulting in a greater depth of necrosis. The purpose of this work is to show a possible correlation between depth of necrosis and the *in vivo* photosensitizer (in this case, Photogem®) photodegradation during PDT. Such correlation allows possibilities for the development of a real time evaluation of the photodynamic action during PDT application. Experiments were performed in a range of fluence (0–450 J/cm^2) at a constant fluence rate of 250 mW/cm^2 and applying different illumination times (0–1800 s) to achieve the desired fluence. A quantity was defined (ψ) as the product of fluorescence ratio (related to the photosensitizer degradation at the surface) and the observed depth of necrosis. The correlation between depth of necrosis and surface fluorescence signal is expressed in ψ and could allow, in principle, a noninvasive monitoring of PDT effects during treatment. High degree of correlation is observed and a simple mathematical model to justify the results is presented. © *2009 American Institute of Physics*. [DOI: 10.1063/1.3116610]

I. INTRODUCTION

Photodynamic therapy (PDT) is a procedure that exploits the consequences from localized oxidative damage caused by photochemical process to produce selective destruction of cells.[1–3] There are three critical elements required for PDT: a photosensitizer (PS), light of proper wavelength to activate the PS, and molecular oxygen in the target tissue.[1] Light interaction with the PS induces the production of highly active species of oxygen, mainly singlet oxygen ($^1O_2$), that mediates localized oxidative damages. These damages lead to tissue necrosis by promoting either direct cell death or vascular damage.[1,4] Clinically, an adequate PDT outcome requires the appropriate combination of those three key elements.

Due to the interdependence of the factors that influence PDT response, some authors suggested that the PS degradation or photobleaching is indicative of an effective administered PDT treatment.[5–8] The PS bleaching rate depends on the PS concentration, the fluence rate, and the availability of molecular oxygen in the tissue.[7] In a situation where surface irradiation is used, light fluence rate decays with tissue depth. That leads to a faster photobleaching rate at the most top layers. As photobleaching occurs, the profile of PS distribution in the tissue is modified and so is the light fluence distribution, as the PS contribution to the attenuation coefficient is reduced.[9]

Since a fraction of the formed reactive oxygen species bleaches the PS molecules and another fraction reacts with tissue molecules, one can assume that the amount of bleached PS is proportional to the amount of tissue damage. In this sense, the correlation of photobleaching to PDT results is a reasonable possibility. If the PS is fluorescent, PS bleaching during PDT can be monitored through fluorescence spectroscopy. The PS fluorescence signal decreases as photobleaching occurs. The purpose of this study is to show that monitoring, at the tissue surface, the induced photobleaching during illumination may be used for a real-time PDT dosimetry and for the prediction of the final depth of necrosis. The photodegradation rate of a hematoporphyrin derivative was evaluated for a sequence of delivered fluences with a constant fluence rate in rat liver. The induced depth of necrosis was measured and a correlation with the measured overall photobleaching was established. A simple theoretical model was developed to explain the overall experimental observations.

It must be emphasized that the observation of photoproducts as well as tissue optical properties variation during the application of PDT is not the goal of our present study.

a)Author to whom correspondence should be addressed. Electronic mail: vander@ifsc.usp.br.

Rather, the final observed variations in PS together with the final observed necrosis are our main objects here.

II. MATERIALS AND METHODS

A. Photosensitizer

The study was performed using a hematoporphyrin derivative, Photogem® (PG), made by Photogem® LLC Co. (Moscow, Russia). It is, in general, described as being chemically similar to Photofrin®.[10] In this sense, both Photogem® and Photofrin® are mixtures of monomers, dimmers, and oligomers of hematoporphyrin derivatives, and first generation PSs.[10,11] The peculiarities of each PS are not relevant for the present study. The 5 mg mL^{-1} stock solutions of Photogem® in 20 mM phosphate buffered saline, *p*H 7.4, were stored in the dark at 4 °C.

B. Animals

Male Wistar rats weighting between 200 and 250 g were used in this study. The animals were maintained according to the guidelines of the Committee on Care and Use of Laboratory Animals of the Brazilian National Research Council and the Commission for Ethics in Research of the Medical School of Ribeirao Preto-University of Sao Paulo (Ribeirao Preto, Brazil).

C. Light source

A diode laser operating at 630 nm (Ceralas®, Ceramoptec, Germany) was used as light source. An optical fiber with a diameter of 300 μm and output lens were used to produce a circular spot with uniform illumination area. The spot size was obtained by controlling the distance between the fiber tip and the target tissue surface. The illumination spot diameter was set as 1 cm for all experiments.

D. Fluorescence spectroscopy system

The fluorescence collection was performed using a system (Spectral-Fluorescence System for Diagnosis of Malignant Tumors, "Spectr-Cluster," v. 2.05m, Cluster Ltd., Moscow, Russia) composed by a Nd^{3+}-doped yttrium aluminum garnet laser emitting at 532 nm (second harmonic emission) as excitation source and a spectrometer to collect fluorescence in the visible to near infrared range (540–850 nm). The excitation laser was coupled to a *Y*-type optical fiber probe (also part of the Spectr-Cluster system). This probe delivers the excitation light through a central optical fiber (diameter $=130$ μm) and collects fluorescence emission from the tissue surface through six fibers (diameter$=100$ μm) arranged around the central one. The output power at the probe tip was about 7 mW to assure that no thermal or photon effects would occur due to the incidence of the fluorescence excitation light during the fluorescence measurement.

Backscattered light from the tissue was about a thousand times more intense than the rest of the fluorescence signal collected by the fibers. To simplify analysis, we used optical filters centered at the excitation wavelength with a long wavelength band pass (above 540 nm) to reduce the intensity of the collected backscattered light. Such attenuation resulted in a backscattering signal that is comparable to the rest of the collected light spectrum. Our attention has been focused in the fluorescence peaks related to the PS and in the autofluorescence previously to injection and not to the backscattered light. The elapsed time for the collection of a single spectrum was less then 10 s.

E. PDT procedure

Normal rat liver was used in these experiments as a model to study the depth of necrosis as a function of fluence. For *in vivo* photodegradation and liver necrosis induction experiments, 27 male Wistar rats were used. Prior to any manipulation, the animals were anesthetized using ketamine 5% (Vetanarcol®, Konig) at the dose of 0.08 mL per 100 g of bodyweight and xylazine 2 g (Coopazine®, Coopers) at the dose of 0.04 mL per 100 g of body weight. A 5 mg mL^{-1} (in 0.9% NaCl) stock solution of the PS was prepared and administered at a concentration of 1.5 mg/kg of body weight through the vena cava, which was made accessible by surgery.[12] Thirty minutes after Photogem® injection,[13] its concentration was confirmed to be at the maximum in the liver via fluorescence spectroscopy. The right lobe of each liver at the center position was then exposed to the light spot.

The experiments were performed using different light fluences (0–450 J/cm^2). Fluence rate was maintained constant (250 mW/cm^2) and exposure time was varied (0–1800 s) to obtain the final applied fluence. Animals were divided into nine subgroups for the different light fluences, with three animals in each subgroup.

After illumination, the animals were sutured to recover from treatment. Thirty hours later, they were killed by an overdose of anesthesia and their livers were removed.[14] The irradiated area was macroscopically evaluated and samples were prepared for histological analysis mainly considering the necrosis aspects and the extension of the depth of necrosis (d_{nec}).

F. Fluorescence procedure

The quantification of the photoactive portion of PS was performed using fluorescence spectroscopy at the illuminated area. The fluorescence spectrum was obtained by placing the probe perpendicularly in contact with the tissue. Total exposure time to the excitation light (532 nm) for every fluorescence collection was less than 10 s, minimizing additional degradation due to excitation light exposure.

Photosensitizer degradation *in vivo* was observed through fluorescence measurements just after the illumination procedure. Fluorescence emission spectra (540–850 nm) were acquired before Photogem® administration, before and after illumination, and at periodical intervals during the therapeutic illumination. For the acquisition of fluorescence spectra, the therapeutic illumination was interrupted for a 10 s period and five fluorescence measurements were collected from different sites inside the illumination spot.

The autofluorescence spectrum obtained before injection was subtracted from the spectrum after injection. The remainder of this procedure is a spectrum with two bands that are mainly related to the PS present in the tissue. In Fig. 1, a

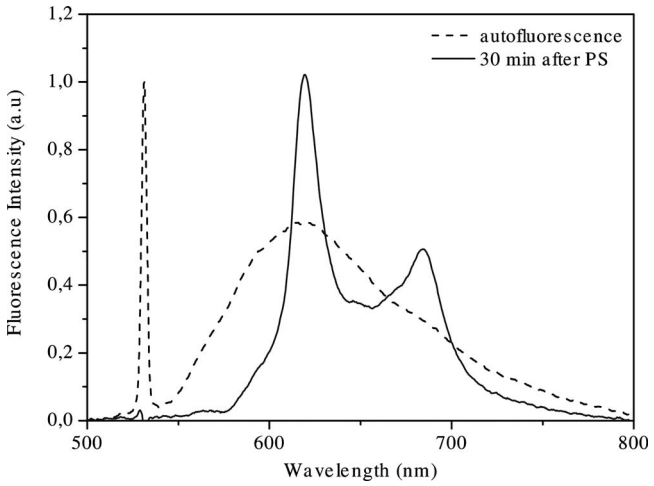

FIG. 1. Fluorescence spectrum of liver without drug (autofluorescence, dashed line) and after 30 min of drug injection (solid line). For the sensitized tissue spectrum, autofluorescence was subtracted. The spectra were normalized to the backscattering peak at 532 nm. Each spectrum is the average of five measurements covering the area of interest.

typical autofluorescence spectrum and the PS fluorescence are shown. As for the fluorescence variation during treatment illumination, we collected spectra from the illuminated area and also from the adjacent region (not illuminated). The nonilluminated area spectra (after autofluorescence subtraction) account for fluorescence variations due to the PS natural pharmacokinetics. Such spectra were subtracted from the PS spectra that were collected from the illuminated area. As a result, the variation due only to PSs phototransformation can be obtained.

G. Degradation rate analyses

The typical fluorescence spectrum for liver (autofluorescence) and for Photogem® in liver before, during, and after irradiation was obtained and normalized by the backscattering peak, observed in 532 nm. The subtraction of autofluorescence was performed to obtain only the PS contribution (i.e., its fluorescence intensity spectrum) as a function of illumination time. Each Photogem® spectrum was normalized by the amplitude at 620 and 680 nm. Five spectra were collected from each area in every condition and data presented in this study are generated by the average amplitudes of these spectra. Error bars represent the standard deviation related to these spectra.

H. Monitoring the thermal effects in the PDT procedure

The possible thermal effect during PDT procedure was monitored on liver as a function of illumination time using a thermistor (Model 120–202 EAJ, Fenwal Electronic, Milford, MA) connected to a data acquisition device. Specific software was developed in LabView® to allow real time visualization of the results. The temperature values were measured in intervals of 1 s.

The obtained results show that the temperature variation during the illumination time reached temperatures of 40–42 °C (data not shown). This type of temperature variation is compatible with observations already reported in the literature.[15] Such final temperature can be seen as indicative of a slight occurrence of hyperthermia, specially for prolonged appliance of illumination.

I. Statistics

Measured fluorescence values and depth of necrosis at liver were statistically compared using an analysis of variance (ANOVA) combined with Student–Newman–Keuls test. For all tests, a P-value of less than 0.05 was considered to be statistically significant.

III. RESULTS AND DISCUSSION

A typical autofluorescence spectrum for the target tissue of this study is presented in Fig. 1. The addition of Photogem® adds the two characteristics bands at 620 and 680 nm already discussed. After autofluorescence subtraction, the spectra show clearly the presence and quantity of the drug. Extracting the precise concentration of PS in the tissue using the fluorescence spectrum[13] is a challenging task due to the optical properties of the medium. Since tissue is a turbid medium, the one-to-one relation between concentration and fluorescence does not hold. We can, however, consider a proportionality relationship such that decreasing fluorescence is associated with photodegradation at the equivalent proportion.

During the illumination procedure, there are continuous changes in the optical properties, which may influence the estimates of photobleaching. We observed that after 20 min of illumination the optical characteristics of the tissue are noticeably different. Before that, changes seem not to be so evident. We always normalized our spectra by the backscattering amplitude, therefore accounting for small variations concerning the coupling of excitation light to the tissue.

The fluence rate used in these experiments resembles the clinical studies using Photogem®.[16] Tromberg *et al.*[17] observed that during PDT using high fluence rate, oxygen depletion occurs with temperature increase. Following their conclusions, if the hyperthermia effect is high enough to contribute to the therapeutic process, the induction of the synergistic effect may have taken place, enhancing tissue damage during PDT.[15] Our results showed that mild hyperthermia (about 40–42 °C) was observed, having only marginal influence for most results. Observed effects due to other factors, rather than PDT, will be discussed within the model discussion subsection.

The obtained depth of necrosis (d_{nec}) as a function of incident light fluences is shown in Fig. 2. Examining the tissue histological slides, we observed a well defined line that separates the necrotic from the normal tissue, therefore making simple the determination of d_{nec}; Figs. 3(a) and 3(b) show a typical line separating both regions. The presence of a well defined separation is a result already explored in detail elsewhere[18] and is related to the threshold dose (D_{th}) below which no permanent damage is observed.[19–21] Considering a superficial illumination given by a fluence value D_0 and a simple exponential decay of the light intensity allows us to write (as an approximation) that

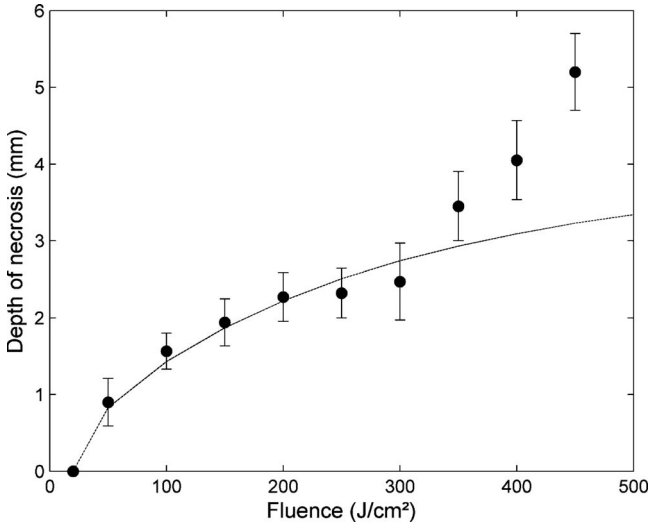

FIG. 2. Experimental depths of necrosis for Photogem® (solid circles) as a function of light fluences (0–450 J/cm^2) with constant fluence rate at 250 mW/cm^2 in different illumination times (0–1800 s). Error bars are standard deviations from measurement of five independent animals. The dashed line corresponds to the result obtained from the constructed model described in the text.

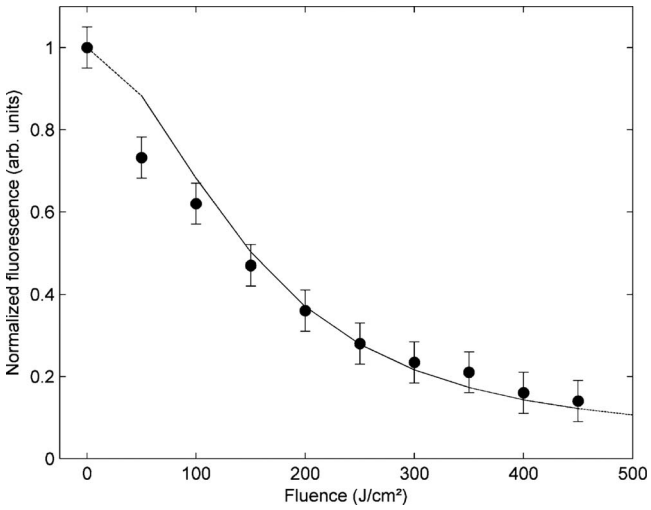

FIG. 4. Normalized experimental FA (degradation) for Photogem® *in vivo* as a function of light fluences (0–450 J/cm^2), using fluence rate at 250 mW/cm^2 and different illumination times (0–1800 s). Error bars on experimental points are taken as the standard deviations from measurement of five independent animals. The dashed line is the obtained result using the model described in the text.

$$d_{\mathrm{nec}} = \delta \ln(D_o/D_{\mathrm{th}}), \tag{1}$$

where δ is the effective penetration depth of light for the considered tissue and D_{th} is the threshold dose. The conventional experiments involving the measurements of d_{nec} versus D_0 show that this approximation, given by Ferreira *et al.*,[18] is an acceptable one.

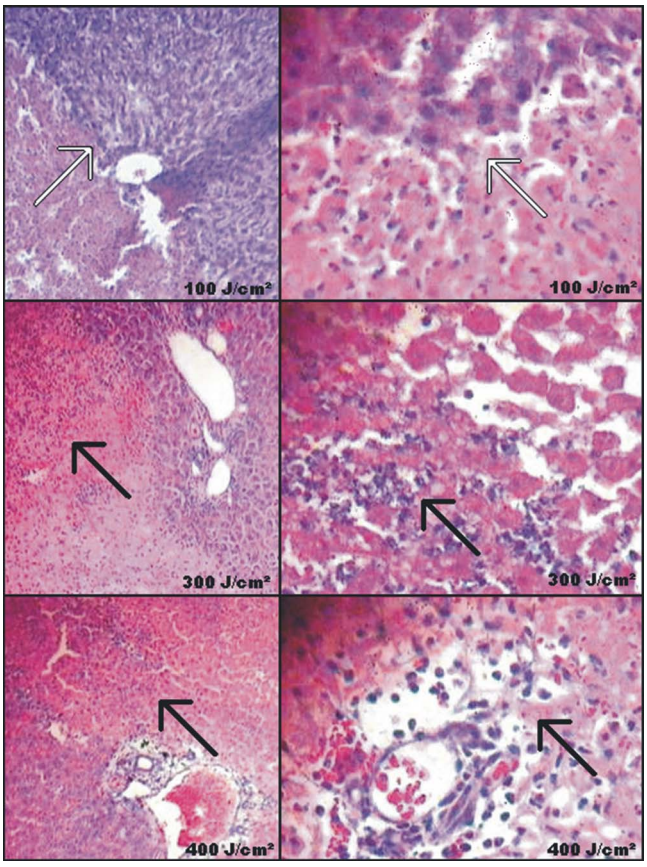

FIG. 3. (Color online) Necrosis slide pictures from illuminated tissue. One can see [at (a) and (b)] a well defined line that separates healthy and necrotic tissue (white arrows) and neutrophils infiltration [in detail at (c) and (d), black arrows], which are indicators of swelling.

The intent of this study is not to analyze the complex model of the photodynamic process. Rather, two quantities are measured and the relation among them is obtained. In writing Eq. (1), we aim to consider a simplified exponential decay. The interpretation for the real observations is carried out using a model that goes beyond a simple exponential decay.

Experimental conditions show good correlation with Eq. (1) for lower fluences ($D_0 < 200$ J/cm^2). For higher fluences, there is a clear deviation from Eq. (1). For the lower fluence values, the line represents the fit using Eq. (1), with $D_{\mathrm{th}} = 15$ J/cm^2, which is within the expected range following reference by Menezes *et al.*[22] For large fluence values, the behavior deviates from the simplified exponential model. Histological examination reveals that the tissues illuminated with fluences above 250 J/cm^2 show a higher presence of neutrophilics, which are indicative of swelling as indicated in Figs. 3(c)–3(f). A predominant large spacing among cells also indicates the presence of edema. Those effects contribute to modifications of the photodynamic reaction and certainly result in variations for the depth of necrosis as a function of light fluences, as observed in Fig. 2, for values of fluence above 300 J/cm^2.

Taking the fluorescence amplitude (FA) as the PS quantification at tissue surface, the relative variation in fluorescence peaks as a function of delivered fluence is shown in Fig. 4. The fluorescence decrease implies an overall production of singlet oxygen, which may be correlated with the overall PDT action. Of course, this explanation relies on the fact that molecular oxygen depletion may be established quite fast if compared with the illumination time. As reported by Henderson *et al.*,[4] a steady-state condition of oxygenation is established just after a few seconds of illumination.

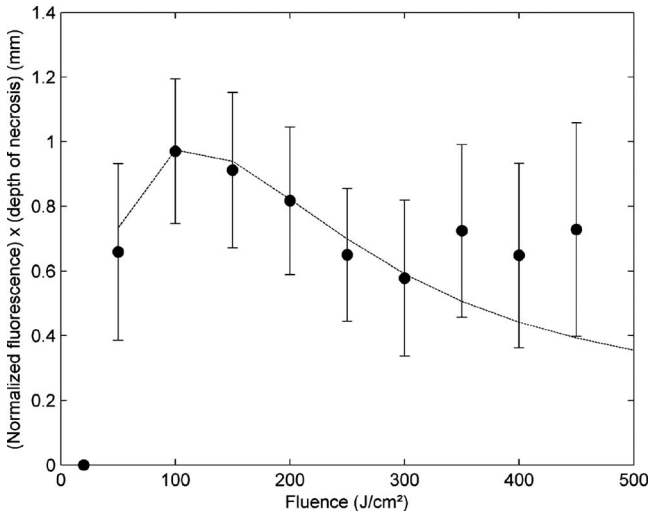

FIG. 5. Experimental fluorescence ratio (degradation) for Photogem® *in vivo* vs depth of necrosis (ψ) as a function of applied light fluences (0–450 J/cm^2) with constant fluence rate at 250 mW/cm^2 and different illumination times (0–1800 s). Error bars are taken as standard deviations from measurement of five independent animals. The dashed line is the result obtained from the constructed model.

Results presented in Figs. 2 and 4 show that there is a clear correlation between the measured quantities, indicating that deeper necrosis is achieved for larger decrease in the PS surface fluorescence. A previous study has been published by Cheung *et al.*[23] presenting *in vivo* correlation of the PS fluorescence and the depth of necrosis. That study, however, is different from the present one, because in their case fluorescence was only measured before illumination as a way to quantify the amount of drug present in the tissue. They found out that there is a correlation between observed fluorescence and the depth of necrosis, as well as between the depth of necrosis and the injected quantity of PS. In our case, the fluorescence is taken during light application and the relative variation observed is mainly attributed to the quantity of photodynamic reaction. Since the purpose is to make it possible to predict the depth of necrosis using measurements of the variations in the surface fluorescence, we defined a variable ψ as the product of the FA and the depth of necrosis. Therefore

$$\psi = (\mathrm{FA}) d_{\mathrm{nec}}, \tag{2}$$

where FA is normalized to the initial value (when $D=0$). This quantity ψ, calculated for our data, is presented as a function of the surface delivered fluence in Fig. 5.

Observe that we apply this quantity ψ only for $D > D_{\mathrm{th}}$, since for $D \leq D_{\mathrm{th}}$, $d_{\mathrm{nec}}=0$ and the search for correlation does not make sense. We calculated the average value of ψ ($\bar{\psi}$) for the investigated light fluence interval, resulting in

$$\bar{\psi} \cong 0.8 \pm 0.2 \ \ (\mathrm{mm}).$$

Because the average is within the variance of the points, we could consider it as a constant. This indicates that, at any moment of the application, since we know the delivered energy/area, the depth of necrosis at that moment is just inversely proportional to the FA measured at the applied surface. Since we used normalized fluorescence, the unit of ψ follows the unit of d_{nec}.

These results are in agreement with explanations offered by Tromberg *et al.*[24] since in the third phase of the photodynamic therapy the regional breakdown of oxygen and nutrient delivery occurs due to vascular collapse, which causes tumor necrosis ("ischemic" stage irreversible). Results indicate that one can actually use ψ to follow the evolution of the depth of necrosis during application of PDT. Of course, it is expected that the value of ψ will vary from one type of tissue to another, as well as with the PS concentration and for different fluence rates. This can eventually be studied and tabulated.

Using our data, the correlation coefficient between the variables depth of necrosis and the inverse of the fluorescence signal ($d_{\mathrm{nec}}=\psi/\mathrm{FA}$) was calculated. A linear regression and correlation model was used.[25] The correlation coefficient (r^2) was evaluated and the value $r^2=0.97$ was obtained (data not shown). The correlation coefficient is a measure of how well trends for the predicted values follow trends in past actual values. Then, it is a measure of how well the predicted values from a forecast model fit with the real values. A correlation coefficient close to one expresses a good strength of the relationship between the predicted values and actual values. The value of 0.97 is a good indication of a direct correlation as expressed in Eq. (2).

A. Modeling the observations

Experimental results show the existence of a correlation between PS photobleaching and depth of necrosis in rat liver. To achieve a better understanding of this experimental observation, a simple theoretical model to evaluate correlation parameter (ψ) was developed. As a simple approach, we can consider that fluence rate distribution changes during PDT due to PS photobleaching, which leads to a change in the PS absorption coefficient.

Photosensitizer bleaching depends on local fluence rate, local oxygen, and PS concentration. In a first approximation, the variation in the PS concentration $C(x,t)$ can be described by the following equation:

$$\frac{d}{dt}C(x,t) = -\beta[\mathrm{O}_2]I(x,t)C(x,t), \tag{3}$$

where β is the degradation rate coefficient and x is depth, or light propagation coordinate, so that $x=0$ corresponds to the surface. The quantity $[\mathrm{O}_2]$ is the oxygen concentration. Oxygen depletion during PDT was taken into consideration in our model as time dependent and is represented by

$$[\mathrm{O}_2] = [\mathrm{O}_2]_0[\exp(-t/\tau_1) + \exp(-t/\tau_2)], \tag{4}$$

with τ_1 and τ_2 adjustable. We can consider that the sum of exponentials represent different contributions to the variation in the oxygen concentration during illumination, as the natural tissue oxygen dynamics and the photodynamic consumption of oxygen.

The PS concentration at a time $t+\Delta t$ is calculated with Eq. (5), where $[\mathrm{O}_2]$ is given by expression (4).

$$C(x,t+\Delta t) = C(x,t) - \beta[O_2]I(x,t)C(x,t)\Delta t. \quad (5)$$

PDT-induced tissue modification is not considered in this model. Therefore, fluence rate $I(x,t)$ depends on local PS concentration and intrinsic tissue optical properties, here considered as time independent. One can write the spatial variation in light intensity as

$$\frac{d}{dx}I(x,t) = -[\sigma C(x,t) + \alpha]I(x,t), \quad (6)$$

where σ is the PS light absorption cross section and α is the tissue intrinsic attenuation coefficient, which is influenced by absorption and scattering.

At a time $t+\Delta t$, fluence rate can be calculated by

$$I(x+\Delta x,t+\Delta t) = I(x,t) - [\sigma C(x,t) + \alpha]I(x,t)\Delta x. \quad (7)$$

To simulate this model numerically, an algorithm was computed in MATLAB®. A set of initial conditions was used to represent a typical liver tissue. Values for σ and α were set to be 1.4 mg^{-1} cm^2 and 0.163 cm^{-1}, respectively. Those values are in agreement with reported values in the literature.[26,27] The value for β (0.000 58 J^{-1} mg^{-1} cm^5) corresponds to the best fitting and there is no source available for comparison. The model results to the measured quantities are shown in Figs. 2 and 4–6 as dashed lines, together with experimental data (as solid circles).

The values for depth of necrosis (d_{nec}) were determined from the curves of fluence as a function of depth (x), considering a threshold dose of 15 J/cm^2, as shown in Fig. 6(b). In the model, τ_1 and τ_2 values were set as, respectively, 290 and 310 s. Those values were adjusted to obtain the best concordance between model and experiment.

The results obtained with this model for the fluence as a function of position are presented in Fig. 6(a), where the local light fluence versus light penetration depth is presented for different times of illumination. Local light fluence for each position is obtained through integration of the local intensity with time ($D=\int I dt$) for the whole illumination period. The crossing of the $D(x,t)$ with the threshold dose D_{th} (here considered as 15 J/cm^2) determines the calculated depth of necrosis for each time of illumination.

In Fig. 6(b), the concentration profiles for PS as obtained from the model are presented for different illumination times. We considered 1 mg/kg as the initial value, since only part of the PS is delivered to the tissue. The depth of necrosis obtained from the model, as in Fig. 6(a) (as the depth for which D_{th} is achieved), is presented as a dashed line in Fig. 2. Similarly, the superficial concentration of PS obtained from the model is plotted as a dashed line in Fig. 4. Comparison between model and experimental data is quite good.

From calculated d_{nec} and superficial PS, ψ is also theoretically obtained as the dashed line in Fig. 5. From the interval of light fluences considered, the average value for ψ is calculated, resulting in $\bar{\psi} \cong 0.65 \pm 0.32$ (mm), close from the value obtained from the data.

Concerning the deviation from the model for fluence values over 250 J/cm^2 (observed in Figs. 2 and 5), we believe that swelling—and the consequent changes in the optical properties due to tissue alteration for these fluence values—

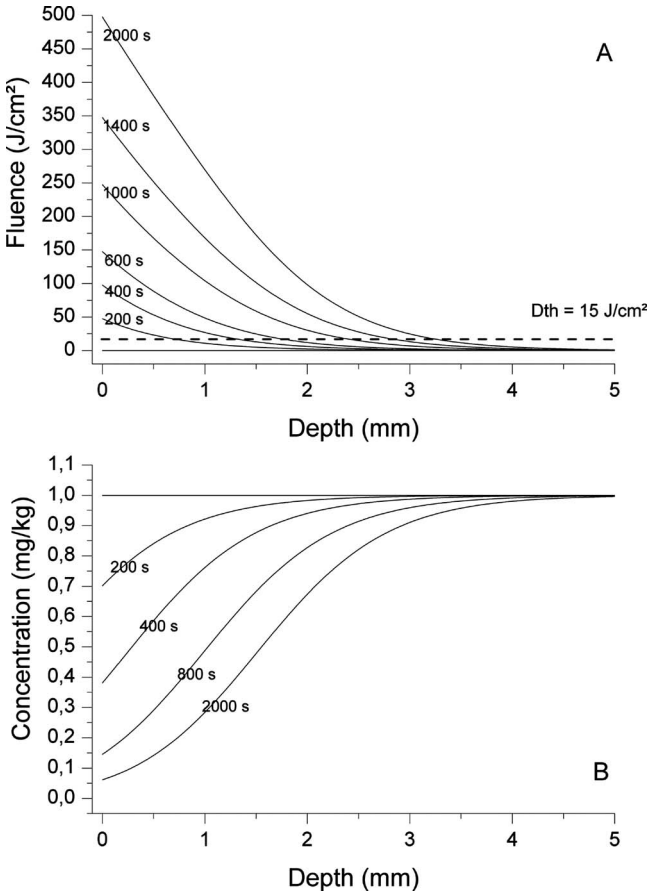

FIG. 6. (a) Theoretical light fluences penetration profiles in tissue during illumination for a constant surface fluence rate and different times of illumination as obtained from the model. The dashed line represents the considered threshold dose to achieve photodynamic effect. (b) Theoretical PS concentration distribution profiles in tissue during illumination for a constant fluence rate and different times of illumination.

are not considered in the model, as mentioned earlier. Furthermore, when tissue undergoes PDT damage, the induced hypoxia and the greater amount of energy delivered to the tissue could interfere with the necrosis establishment.

In this scenario, deeper necroses for the highest fluences are quite expected as observed. Such increase is also responsible for the increase in the actual ψ values when compared to those of the model prediction for fluences well above 250 J/cm^2. Therefore, if such tissue properties variation could be taken into account, it would certainly be possible to match prediction and actual values for the high fluence region much better.

Nevertheless, this model can be considered as a good approach, which takes the main PDT mechanisms into account, and with reasonable representation of its actual results. The agreement between prediction model and experimental data below 250 J/cm^2 shows that our considerations seem to be true especially for low fluence values, where PDT facts and mechanisms are better under control. High fluences, however, seem to promote additional phenomena that interfere with both photobleaching and depth of necrosis. This interference could be elucidated by additional studies.

On the other hand, high fluence values are usually avoided exactly to prevent thermal damage effects. There-

fore, correlation between surface fluorescence (degradation) information and depth of necrosis might still contribute to clinical dosimetry of PDT. Nonetheless, the final aim of this study was to present a practical model that—even known to be not complete—could be applied to improve PDT. This improvement can enhance PDT outcome for patients while more complete understanding and description of PDT effects are achieved.

IV. CONCLUSIONS

We demonstrated the existence of a well established correlation between surface fluorescence and depth of necrosis during PDT for an experimental model using healthy rat liver. In this sense the work here presented complements others already published.[1,4,5,28–31] A model taking into account the main effects occurring during PDT applications allows us to understand the main facts for fluences lower than 250 J/cm^2. Differences observed for higher fluences can be qualitatively explained based on a hypothesis of the establishment of a balance between photon absorption by the PS and the rate of molecular oxygen depletion. The photodegradation observed by fluorescence at the illuminated surface offers a strong correlation with depth of necrosis. Because implicit dosimetry relies on a surrogate indicator of damage to measure the photodynamic effect, rather than calculation of dose, it may be that the real time monitoring of the PS fluorescence during PDT will allow the prediction of depth of necrosis and contribute to a real time dosimetry.

ACKNOWLEDGMENTS

The authors would like to acknowledge Maristela Dutra-Correa, Ruy C. M. C. Ferraz, Paulino R. Villas Boas, and Juliana Ferreira for the technical and computational assistance and to Brazilian agencies CAPES and FAPESP for the financial support to perform this study.

[1]B. W. Henderson, T. M. Busch, and J. W. Snyder, Lasers Surg. Med. **38**, 489 (2006).
[2]R. R. Allison, V. S. Bagnato, R. Cuenca, G. H. Downie, and C. H. Sibata, Future Oncol. **2**, 53 (2006).
[3]R. R. Allison, C. Sibata, G. H. Downie, and R. Cuenca, Photodiag Photodyna Ther **3**, 214 (2006).
[4]B. W. Henderson, T. M. Busch, L. A. Vaughan, N. P. Frawley, D. Babich, T. A. Sosa, J. D. Zollo, A. S. Dee, M. T. Cooper, D. A. Bellnier, W. R. Greco, and A. R. Oseroff, Cancer Res. **60**, 525 (2000).
[5]M. J. Niedre, A. J. Secord, M. S. Patterson, and B. C. Wilson, Cancer Res. **63**, 7986 (2003).
[6]B. C. Wilson, M. S. Patterson, and L. Lilge, Lasers Med. Sci. **12**, 182 (1997).
[7]D. J. Robinson, H. S. de Bruijn, N. van der Veen, M. R. Stringer, S. B. Brown, and W. M. Star, Photochem. Photobiol. **67**, 140 (1998).
[8]D. J. Robinson, H. S. de Bruijn, N. van der Veen, M. R. Stringer, S. B. Brown, and W. M. Star, Photochem. Photobiol. **69**, 61 (1999).
[9]T. J. Farrell, R. P. Hawkes, M. S. Patterson, and B. C. Wilson, Appl. Opt. **37**, 7168 (1998).
[10]A. F. Mironov, A. N. Nizhnik, and A. Y. Nockel, J. Photochem. Photobiol. B: Biol. **4**, 297 (1990).
[11]P. Company, *Photogem*, in *Russian Pharmacopoeia*. 10/02/1999, Ministry of Health of Russian Federation: Russian.
[12]P. F. C. Menezes, H. Imasato, J. Ferreira, V. S. Bagnato, and J. R. Perussi, Laser Phys. **17**, 461 (2007).
[13]C. A. Melo, C. Kurachi, C. Grecco, C. H. Sibata, E. Castro, and O. Silva, J. Photochem. Photobiol., B **73**, 183 (2004).
[14]J. Ferreira, *Faculdade de Medicina de Ribeirão Preto-FMRP* (Universidade de São Paulo–USP, Ribeirão Preto, 2003), p. 99.
[15]A. Orenstein, G. Kostenich, H. Tsur, L. Kogan, and Z. Malik, Cancer Lett. **93**, 227 (1995).
[16]V. S. Bagnato, C. Kurachi, J. Ferreira, L. G. Marcassa, C. H. Sibata, and R. R. Allison, Photodiag Photodyna Ther **2**, 107 (2005).
[17]B. J. Tromberg, A. Orenstein, S. Kimel, S. J. Barker, J. Hyatt, J. S. Nelson, and M. W. Berns, Photochem. Photobiol. **52**, 375 (1990).
[18]J. Ferreira, L. T. Moriyama, C. Kurachi, and C. Sibata, Laser Phys. Lett. **4**, 469 (2007).
[19]L. I. Grossweiner, Lasers Surg. Med. **11**, 165 (1991).
[20]M. S. Patterson, B. C. Wilson, and R. Graff, Photochem. Photobiol. **51**, 343 (1990).
[21]S. G. Bown, C. J. Tralau, P. D. Smith, D. Akdemir, and T. J. Wieman, Br. J. Cancer **54**, 43 (1986).
[22]P. F. C. Menezes, J. Ferreira, V. S. Bagnato, H. Imasato, and J. R. Perussi, Laser Phys. **17**, 461 (2007).
[23]R. Cheung, M. Solonenko, T. M. Busch, F. Del Piero, M. E. Putt, S. M. Hahn, and A. G. Yodh, J. Biomed. Opt. **8**, 248 (2003).
[24]B. J. Tromberg, S. Kimel, A. Orenstein, S. J. Barker, J. Hyatt, J. S. Nelson, W. G. Roberts, and M. W. Berns, J. Photochem. Photobiol., B **5**, 121 (1990).
[25]A. L. Edwards, *Introduction to Linear Regression and Correlation*. An Introduction to Linear Regression and Correlation Vol. 36. (Freeman, San Francisco, CA, 1976), p. 213.
[26]J. C. Finlay, S. Mitra, M. S. Patterson, and T. H. Foster, Phys. Med. Biol. **49**, 4837 (2004).
[27]P. Parsa, S. L. Jacques, and N. S. Nishioka, Appl. Opt. **28**, 2325 (1989).
[28]K. Langmack, R. Mehta, P. Twyman, and P. Norris, J. Photochem. Photobiol., B **60**, 37 (2001).
[29]H. W. Wang, M. E. Putt, M. J. Emanuele, D. B. Shin, E. Glatstein, A. G. Yodh, and T. M. Busch, Cancer Res. **64**, 7553 (2004).
[30]T. M. Busch, S. M. Hahn, S. M. Evans, and C. J. Koch, Cancer Res. **60**, 2636 (2000).
[31]T. H. Foster, R. S. Murant, R. G. Bryant, R. S. Knox, S. L. Gibson, and R. Hilf, Radiat. Res. **126**, 296 (1991).